Feasibility of Higher-Order Differential Ion Mobility Separations Using New Asymmetric Waveforms

Alexandre A. Shvartsburg,*,† Stefan V. Mashkevich,‡ and Richard D. Smith†

Biological Sciences Division, Environmental Molecular Sciences Laboratory, Pacific Northwest National Laboratory, MS K8-98, 3335 Q Avenue, Richland, Washington 99352, and Schrödinger, 120 West 45th Street, New York, New York 10036-4041

Received: September 20, 2005; In Final Form: November 16, 2005

Technologies for separating and characterizing ions based on their transport properties in gases have been around for three decades. The early method of ion mobility spectrometry (IMS) distinguished ions by absolute mobility that depends on the collision cross section with buffer gas atoms. The more recent technique of field asymmetric waveform IMS (FAIMS) measures the difference between mobilities at high and low electric fields. Coupling IMS and FAIMS to soft ionization sources and mass spectrometry (MS) has greatly expanded their utility, enabling new applications in biomedical and nanomaterials research. Here, we show that time-dependent electric fields comprising more than two intensity levels could, in principle, effect an infinite number of distinct differential separations based on the higher-order terms of expression for ion mobility. These analyses could employ the hardware and operational procedures similar to those utilized in FAIMS. Methods up to the 4th or 5th order (where conventional IMS is 1st order and FAIMS is 2nd order) should be practical at field intensities accessible in ambient air, with still higher orders potentially achievable in insulating gases. Available experimental data suggest that higher-order separations should be largely orthogonal to each other and to FAIMS, IMS, and MS.

Approaches to separation of ion mixtures and characterization of ions in the gas phase based on ion mobility are becoming commonplace in analytical chemistry. The key advantage of gas-phase separations over condensed phase methods is the exceptional speed enabled by rapid molecular motion in gases. This inherent benefit is made increasingly topical by the growing focus of analytical technology on higher throughput. Since their first demonstration a decade ago,[1−3] instrumental platforms combining electrospray ionization (ESI) or matrix-assisted laser desorption ionization (MALDI) sources with ion mobility separations and mass-spectrometry (MS) have undergone a sustained development that has improved their resolution and sensitivity to the levels demanded by practical applications.[4−10] Recent commercial introduction of such systems[11−14] is expanding interest in ion mobility/MS, particularly for analyses of complex biological samples such as proteolytic digests and lipids, nucleotides, and metabolites.[15−24]

Single-stage ion mobility spectrometry (IMS) was investigated since the 1970s,[25−27] with a noteworthy development of ESI/IMS in 1980s.[28] In IMS, ions drift through a nonreactive buffer gas under the influence of a modest electric field. The drift velocity (v) in the field of intensity E is determined by ion mobility (K):

$$v = E \times K(E) \tag{1}$$

For consistency, measured mobilities are normally converted to reduced values K_0 by adjusting the buffer gas temperature (T, Kelvin) and pressure (P, Torr) to standard (STP) conditions:

$$K_0 = K(P/760) \times (273.15/T) \tag{2}$$

The mobility of an ion always depends on the electric field. This dependence may be expressed as an infinite series of even powers over E/N, where N represents the gas number density:[9,29]

$$K_0(E) = K_0(0)[1 + a(E/N)^2 + b(E/N)^4 + c(E/N)^6 + d(E/N)^8 + e(E/N)^{10} + ...] \tag{3}$$

Rigorously, IMS measures $K(E)$ at a particular E. However, typically E/N is under ∼20 Td, for example, ∼5−16 Td in MS/IMS/MS systems[1,2,4,7,15] operated at low $P \approx 1-5$ Torr and a lower ∼1−4 Td in IMS[28] and IMS/MS[5,6,12] with "high" $P \approx 150-760$ Torr. Under those conditions, $K(E)$ varies[30−33] by $< \sim 1\%$. Thus, although $K(E)$ could be revealed by IMS experiments at very low $P \approx 0.03-0.5$ Torr,[34−36] in practice IMS essentially separates ion mixtures by zero-field mobility $K_0(0)$.

The mobility of an ion is related to its size and thus to its mass m (especially within classes of homologous or chemically/structurally similar species), meaning that the orthogonality between IMS and MS analyses is limited. For example, ions of the same charge state z follow certain trend lines in IMS/MS plots, depending on the chemical composition and compound type. In particular, trend lines have been described for atomic nanoclusters[37−42] (including carbon, semiconductor, and metal species) and biomolecules (including peptides, lipids, and nucleotides).[16−21,43,44] Using ESI, complex biological analytes such as tryptic digests generally yield ions with a distribution of z that have different trend lines in IMS/MS space.[6,7,16] While this increases the apparent 2-D peak capacity of IMS/MS, the

* Corresponding author. E-mail: alexandre.shvartsburg@pnl.gov.
† Pacific Northwest National Laboratory.
‡ Schrödinger.

10.1021/jp055349t CCC: $33.50
Published on Web 02/07/2006

correlation between ion mobility and mass is a fundamental limitation of IMS/MS methodology.

This limitation has been one driver behind the recent development of field asymmetric waveform IMS (FAIMS),[13,14,30−33] which separates ions by differential mobility as a function of electric field using a time-dependent field $E(t)$. In this field, an ion drifts with the mean velocity:

$$\langle v\rangle = [\int_{t_0}^{t_0+\Delta t} K(E)E(t)\,dt]/\Delta t \quad (4)$$

The limits of integrals below are also t_0 and $(t_0 + \Delta t)$, but are dropped for conciseness. With $K(E)$ defined by eq 3, eq 4 expands into:

$$\langle v\rangle = K(0) \times [\int E(t)\,dt + (a/N^2)\int E^3(t)\,dt + (b/N^4)\int E^5(t)\,dt + (c/N^6)\int E^7(t)\,dt + (d/N^8)\int E^9(t)\,dt + (e/N^{10})\int E^{11}(t)\,dt + ...]/\Delta t \quad (5)$$

This motion may be offset using a constant field E_C that pulls ions back with the velocity v_C:

$$v_C \approx E_C \times K(0) \quad (6)$$

A FAIMS separation may be achieved by any periodic asymmetric function $E(t)$ for which:

$$\int E(t)\,dt = 0; \quad \int E^3(t)\,dt \neq 0 \quad (7)$$

with Δt now being the period of $E(t)$. Condition (7) cancels the 1st (but not the 2nd) term of polynomial (5). Setting $\langle v\rangle = -v_C$, one finds from eqs 5 and 6:

$$E_C \approx -[(a/N^2)\int E^3(t)\,dt + (b/N^4)\int E^5(t)\,dt + (c/N^6)\int E^7(t)\,dt + (d/N^8)\int E^9(t)\,dt + (e/N^{10})\int E^{11}(t)\,dt + ...]/\Delta t \quad (8)$$

The independence of E_C (compensation field) from $K(0)$ allows FAIMS to disperse ions by the sum of 2nd and further terms of eq 3, regardless of the absolute mobility. At a sufficiently low peak amplitude of $E(t)$ (known as the "dispersion field", E_D), E_C is mostly determined by the leading term of eq 8, that is, the coefficient a. Subsequent terms (especially the 2nd) affect the FAIMS response at higher E_D, which in some cases[31] allows for the measurement of coefficient b. Still, FAIMS separations are mainly controlled by the value of a; differences between b, c, ... create no significant orthogonality and so are of little practical utility. This is parallel to IMS where the value of a could be measured, but is nearly immaterial to the separation, as described above.

Condition (7) is satisfied by an infinite number of $E(t)$ functions. However, FAIMS resolution and specificity are optimized by maximizing $\langle v\rangle \propto \int E^3(t)\,dt/\Delta t$ (ignoring higher-order terms).[45] That is ideally achieved by a "rectangular" waveform,[45,46] where $E(t)$ switches between segments of "high field" (E_D) over a time t_D and "low field" (E_L) in the opposite direction over a time t_L. The criterion $\int E(t)\,dt = 0$ of condition (7) requires E_D/E_L (known as the "high-to-low" ratio f) to equal $-t_L/t_D$. This quantity may mathematically vary between 1 and $+\infty$, but the best FAIMS performance is provided[47]

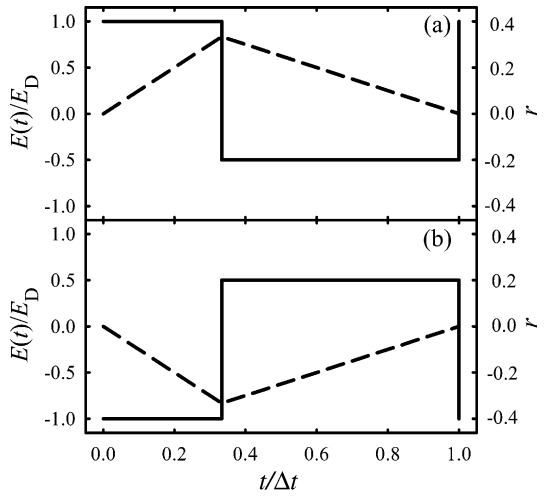

Figure 1. Optimized time-dependent electric fields for FAIMS (solid lines, left axis) and the ideal ion trajectories in those fields (dashed lines, right axis). There are two possible polarities: (a) and (b).

by $f = 2$, when

$$E(t) = E_D\,\{t \in [0; \Delta t/3]\}; \quad E(t) = -E_D/2\,\{t \in [\Delta t/3; \Delta t]\} \quad (9)$$

(Figure 1a) or a waveform of inverted polarity (Figure 1b). Equation 9 produces:

$$\langle v\rangle = K(0)[(a/N^2){E_D}^3/4 + 5(b/N^4){E_D}^5/16 + O(c{E_D}^7/N^6)]/\Delta t \quad (10)$$

$$E_C = -[(a/N^2){E_D}^3/4 + 5(b/N^4){E_D}^5/16 + O(c{E_D}^7/N^6)]/\Delta t \quad (11)$$

Model trajectories for ions experiencing a period of $[E(t) + E_C]$ by eqs 9 and 11 are plotted in Figure 1. This calculation does not account for ion diffusion or space-charge effects, which is acceptable for comparing trajectories induced by different $E(t)$: the form of $E(t)$ influences the diffusion only slightly through high-field and anisotropic terms and does not affect Coulomb repulsion.[46] All of the above is well-known in FAIMS theory[46−48] and supported by experiments.

In operation, FAIMS conceptually resembles a quadrupole mass filter. Ions are moved through a gap between two electrodes (the analytical gap) by a gas flow.[49] A voltage waveform applied to this electrode pair creates the field $[E(t) + E_C]$ across the gap. Parallel planar,[50] coaxial cylindrical,[49,51] and concentric spherical[52] electrode geometries (and their combinations[10,13]) have been considered, and other configurations are possible. At any given E_C, ideally only one species with $K(E)$ yielding $\langle v\rangle = v_C$ is balanced in the gap and transmitted. Other ions drift across the gap and are eventually neutralized on an electrode. Scanning E_C produces a spectrum of the ion mixture.[49] Fundamentally, the value of a is not related to m as closely as $K(0)$; in particular, a may be both positive and negative,[33] while K is always positive. As a result, FAIMS is generally more orthogonal to MS than IMS. For example, FAIMS and MS separations for tryptic peptides are independent,[24,53] while IMS and MS are substantially correlated.[6,7,16] This orthogonality is a major advantage of FAIMS/MS over IMS/MS.

This prompts the question as to whether fundamentally novel ion mobility separations might exist. To be useful, the separations would have to be substantially orthogonal to both FAIMS

and IMS or outperform them in other respects. Here, we show that, in principle, there is an infinite number of mutually orthogonal separations based on the 3rd and higher terms of $K(E)$ expansion (3) just as IMS and FAIMS are based on the 1st and 2nd terms, respectively.

Fundamental Feasibility of Higher-Order Differential Ion Mobility Separations (HODIMS)

First, we prove the physical possibility of separations based on the terms of eq 3 beyond any chosen order. Solutions for $E(t)$ will be sought as a number (k) of discrete field settings E_i ($i = 1, k$) applied over time segments t_i, which for $k = 2$ reduces to ideal FAIMS rectangular waveforms. To simplify the mathematics, all E_i and t_i values are scaled so that $E_1 = 1$ and $t_1 = 1$.

To achieve separations based on the $b(E/N)^4$ and higher terms of eq 3, one must cancel both the 1st and the 2nd terms of eq 5 without canceling the 3rd term (proportional to $\int E^5(t)\,dt$). This is impossible using a "rectangular" ($k = 2$) waveform with any f value. Indeed, the system

$$\int E(t)\,dt = 0; \quad \int E^3(t)\,dt = 0 \tag{12}$$

reduces to a cubic equation ($f^3 - f = 0$) with roots $f = \{-1; 0; 1\}$; that is, the waveform does not exist ($f = \{0; 1\}$) or is symmetric ($f = -1$), and trivially $\int E^{2n-1}(t)\,dt = 0$ for any separation order n.

However, a $E(t)$ comprising three different field settings may satisfy the condition (12), yet yield $\int E^5(t)\,dt \neq 0$. Moreover, system (12) contains two equations, but four variables $\{t_2; E_2; t_3; E_3\}$. Hence, an infinite number of such waveforms exist. Similar to the FAIMS case, the optimum $E(t)$ would maximize $\int E^5(t)\,dt/\Delta t$. The two equations of condition (12) allow t_3 and E_3 to be expressed in terms of t_2 and E_2; then the function to be maximized is:

$$\int E^5(t)\,dt/\Delta t = \frac{1 + t_2 E_2^{\,5} - [(1 + t_2 E_2^{\,3})^2/(1 + t_2 E_2)]}{1 + t_2 + \sqrt{(1 + t_2 E_2)^3/(1 + t_2 E_2^{\,3})}} \tag{13}$$

The maximum of function (13) is located at $\{t_2 = 2; E_2 = (\sqrt{5} - 1)/4 \cong 0.309\}$, yielding $\{t_3 = 2; E_3 = -(\sqrt{5} + 1)/4 \cong -0.809\}$. Because the order of t_2 and t_3 is not fixed, this solution produces two waveforms that are mirror images with respect to the time inversion (Figure 2a and b):

$$E(t) = E_D\,\{t \in [0; \Delta t/5]\}; \quad E_2 E_D\,\{t \in [\Delta t/5; 3\Delta t/5]\}; \quad E_3 E_D\,\{t \in [3\Delta t/5; \Delta t]\} \tag{14}$$

$$E(t) = E_D\,\{t \in [0; \Delta t/5]\}; \quad E_3 E_D\,\{t \in [\Delta t/5; 3\Delta t/5]\}; \quad E_2 E_D\,\{t \in [3\Delta t/5; \Delta t]\} \tag{14'}$$

The polarities of both may also be inverted. The maximum of eq 13 is 1/16, thus:

$$\langle v \rangle = K(0)[(b/N^4)E_D^{\,5}/16 + O(cE_D^{\,7}/N^6)]/\Delta t \tag{15}$$

$$E_C = -[(b/N^4)E_D^{\,5}/16 + O(cE_D^{\,7}/N^6)]/\Delta t \tag{16}$$

That is, E_C is rigorously independent of both the absolute mobility $K(0)$ and the coefficient a, creating, in effect, a 3rd order IMS that separates ions primarily by the value of b. The waveforms (14) also yield nonzero higher-order terms in eq 5 involving coefficients $\{c, d, ...\}$ that would influence the results, especially at higher E_D where the $O(cE_D^{\,7}/N^6)$ term grows in importance. This effect is parallel to that found in IMS and FAIMS, as described above.

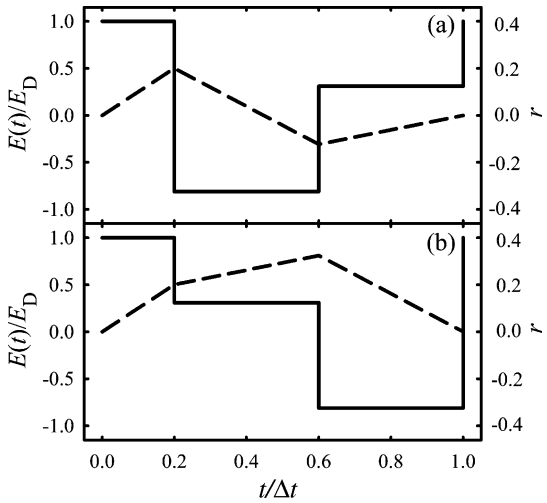

Figure 2. Same as Figure 1 for 3rd order differential IMS separating ions by coefficient b (only one polarity is shown for each waveform).

Waveforms (14) and (14′) are not equivalent because ion trajectories in the field of $[E(t) + E_C]$ during the $E(t)$ period differ, even though the final displacements are null in both cases (Figure 2a and b). Still, maximum amplitudes of ion oscillation during the period (Δr) are equal. This parameter determines the "tightness" of a given gap width and thus is critical in the design of FAIMS separations[47] and also HODIMS, as discussed below. As a corollary of eq 1:

$$\Delta r = C_E K(E) E_D \Delta t \tag{17}$$

where C_E is a numerical coefficient ($0 < C_E < 1$) that depends on the waveform profile. For eqs 14/14′, $C_E \cong 0.3236$, which is slightly lower than $C_E = 1/3$ in FAIMS.

This approach could be used to design $E(t)$ for IMS of still higher orders. For the 4th order separation, primarily by coefficient c, a waveform must satisfy:

$$\int E(t)\,dt = 0; \quad \int E^3(t)\,dt = 0; \quad \int E^5(t)\,dt = 0; \quad \int E^7(t)\,dt \neq 0 \tag{18}$$

Setting eq 13 to zero yields only the solutions that annihilate $\int E^{2n+1}(t)\,dt$ for all n, so no waveform with $k \leq 3$ meets condition (18). Seeking an $E(t)$ with $k = 4$ provides six variables $\{t_2; E_2; t_3; E_3; t_4; E_4\}$ to satisfy three equations in eq 18. Again, this can be achieved by an infinite multiplicity of $E(t)$, but the number of free variables has prevented a truly a priori optimization. However, the 1:2 optimum ratio of t_1:t_2 in FAIMS (i.e., the 2nd order IMS) and the 1:2:2 ratio of t_1:t_2:t_3 for $n = 3$ appear to reveal a trend, extrapolating to the 1:2:2:2 ratio of t_1:t_2:t_3:t_4 for $n = 4$. While we cannot rigorously prove this recipe for maximizing $\int E^7(t)\,dt$, the results below support its verity. The constraint leaves three variables $\{E_2; E_3; E_4\}$ for three equations in (18), which defines a unique solution. Numerically, we obtain $\{-0.223; 0.623; -0.901\}$. Because $t_2 = t_3 = t_4$, which value is assigned to which of E_2, E_3, and E_4 is immaterial. Combinatorial rules allow $(n - 1)! = 6$ different waveforms with two polarities each, making three pairs of $E(t)$ that are identical with respect to the time inversion (Figure 3a/b, c/d,

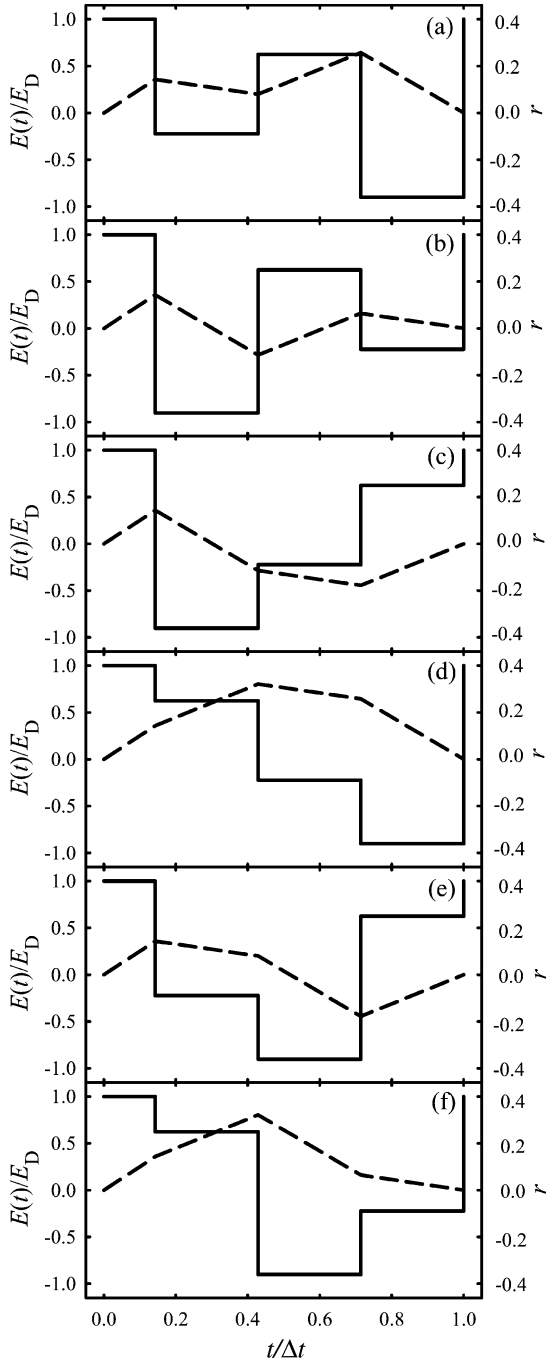

Figure 3. Same as Figure 3 for $n = 4$, with ions separated by coefficient *c*.

e/f). Any of these pairs results in:

$$E_C = -[(c/N^6)E_D{}^7/64 + O(dE_D{}^9/N^8)]/\Delta t \qquad (19)$$

that is, the separation is independent of $K(0)$, *a*, and *b*. By comparison of eqs 11, 16, and 19, the numerical coefficient with the leading term at separation order *n* equals 4^{1-n}: 1/4 for $n = 2$, 1/16 for $n = 3$, and 1/64 for $n = 4$. This trend supports the above assertion of a 1:2:2:2 ratio for waveform segment durations. The six ideal $E(t)$ forms are not equivalent and produce different ion trajectories (Figure 3). Unlike for $n = 3$ above, those may have different Δr values ($C_E \cong 0.257$ for a and b or $C_E \cong 0.321$ for c−e), which would result in a different instrumental response.

For the 5th order separation independent of $K(0)$, *a*, *b*, and *c*, $E(t)$ must satisfy:

$$\int E(t)\,dt = 0; \quad \int E^3(t)\,dt = 0; \quad \int E^5(t)\,dt = 0; \quad \int E^7(t)\,dt = 0; \quad \int E^9(t)\,dt \neq 0 \qquad (20)$$

These conditions can be met by an infinite number of waveforms with $k \geq 5$. Assuming $t_1{:}t_2{:}t_3{:}t_4{:}t_5 = 1{:}2{:}2{:}2{:}2$ by the above-formulated rule, a numerical optimization of four variables $\{E_2; E_3; E_4; E_5\}$ for maximum $\int E^9(t)\,dt$ yields $\{0.174; -0.500; 0.770; -0.940\}$. Again, as $t_2 = t_3 = t_4 = t_5$, these values may be freely permuted within the $\{E_2; E_3; E_4; E_5\}$ set, creating $(n-1)! = 24$ different $E(t)$ with two polarities each, of which 12 are nonidentical with respect to the time inversion (Figure 4a−l). Any of them provides separations primarily by coefficient *d*:

$$E_C = -[(d/N^8)E_D{}^9/256 + O(eE_D{}^{11}/N^{10})]/\Delta t \qquad (21)$$

with the leading term coefficient equal to 1/4 of 1/64 in eq 19, following the rule asserted above. Again, these waveforms produce ion trajectories with different Δr values ($C_E \cong 0.209$, $C_E \cong 0.282$, or $C_E \cong 0.320$) and so would yield a different instrumental response.

The present optimization approach involves $(n-1)$ variables, so maximizing $\int E^{2n-1}(t)\,dt$ is a growing challenge at higher *n*. We have not examined $n > 5$, but conceptually the procedure allows designing $E(t)$ to cancel any number of leading terms in eq 3, enabling separations of arbitrarily high order.

It may be of concern that the series in eq 3 has a finite radius of convergence (E^*).[29] By eq 6-1-58b of ref 29, the convergence condition is $|a|(E/N)^2 < 1$. E^* then depends on the ion, generally decreasing for smaller ions with larger $|a|$. For example, for 17 amino acid ions in air,[31] the measured *a* (below in 10^{-6} Td^{-2}) ranges from 1.27 to 17.4, allowing $E^* \sim 240-900$ Td. The values of $|a|$ for peptides are normally lower than those for single amino acids; hence, E^* would be yet higher. For smaller ions, $|a|$ (in air) and corresponding E^* are, for example, 0.25−31.4 (∼180−2000 Td) for 16 ketone monomers and dimers,[33] 5.22−15.1 (∼260−440 Td) for 9 small organic ions,[54] and 0.27−5.09 (∼440−1900 Td) for 17 organophosphorus compounds.[55] As discussed below, the electrical breakdown threshold in HODIMS for air or N_2 at 1 atm is $E_{BR}/N \approx 160-220$ Td (depending on the instrumental parameters). Thus, $E^* \gg E_{BR}/N$ for all cases considered except one (H^+acetone with $a = 31.4$),[33] and E^* would not normally be reached in HODIMS using air or N_2 media.

Further, a theoretical divergence of eq 3 would not affect the feasibility of HODIMS. This is because the method of *n*th order requires only the cancellation of $(n-1)$ leading terms of eq 3, and each of those is of course finite regardless of whether the series converges. However, the separation parameter reflecting the sum of all nonannihilated terms of eq 3 may have no relation to the pertinent higher-order coefficient (e.g., *b* for $n = 3$). To measure the actual *b*, *c*, *d*, ... using HODIMS with $n = 3, 4, 5, \ldots$, one would have to study the limiting behavior with decreasing E/N, as is presently done to determine true $K(0)$ in IMS and *a* in FAIMS. Doing that accurately may in some cases prove impossible, because the magnitude of the HODIMS (or FAIMS) effect drops and thus the error margin increases with decreasing E/N. In any event, we envision the major utility of HODIMS not in extracting the coefficients in eq 3, but in providing new gas-phase separations, an objective on which the issue of convergence of eq 3 has no bearing.

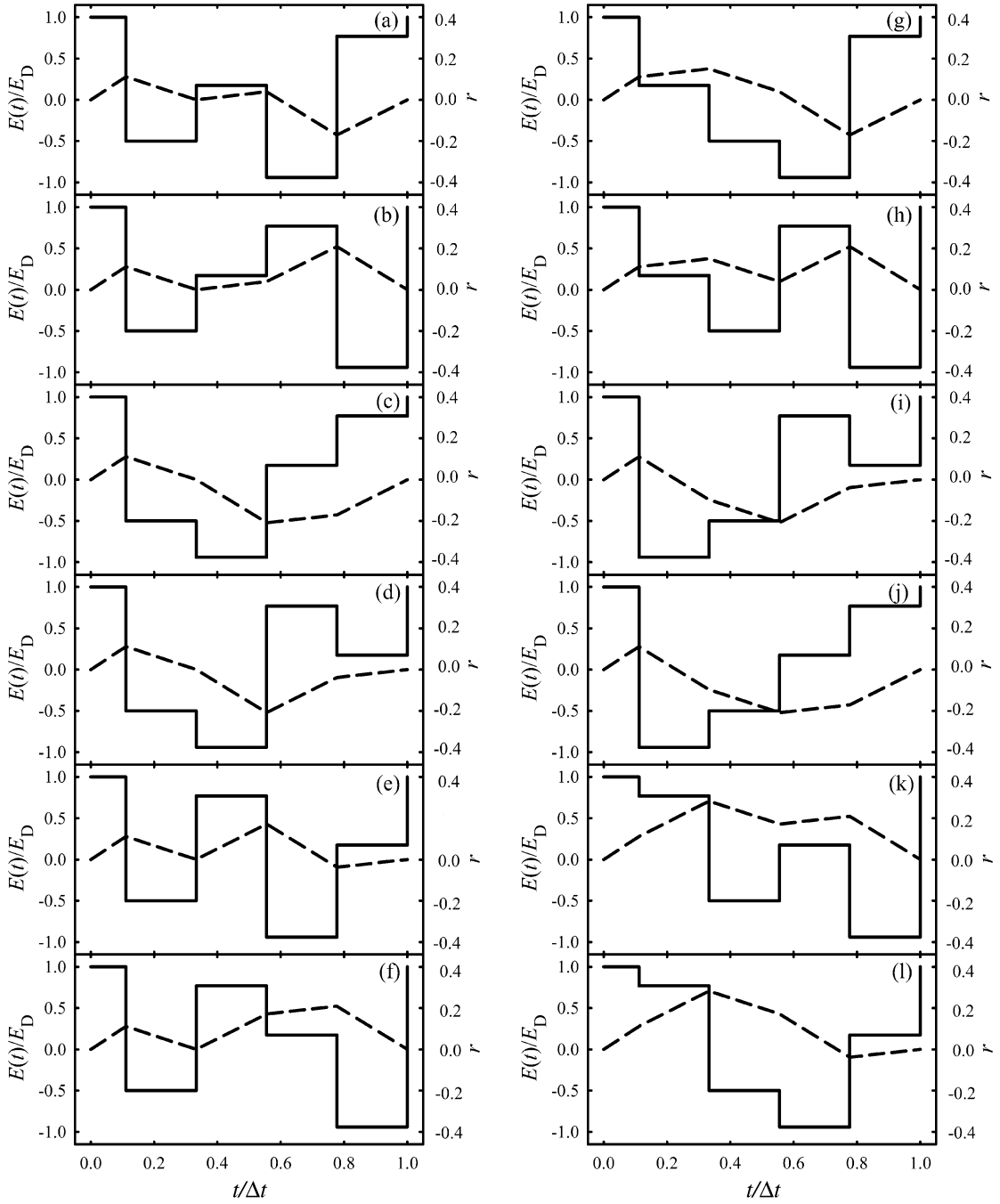

Figure 4. Same as Figure 3 for $n = 5$, with ions separated by coefficient *d*. Twelve out of 24 total waveforms are shown; the other 12 could be obtained via time inversion.

Practical Aspects of Implementing Higher-Order Separations

With the theoretical feasibility of HODIMS established, we now discuss the major issues associated with their experimental implementation.

Mechanical Embodiment. Separation in HODIMS could be effected by the filtering mechanism used in FAIMS, whereby ions are injected between two electrodes that carry voltages generating the desired time-dependent electric field between, and species with unbalanced trajectories are neutralized on one of the electrodes. Again, ions could be pushed through the gap by gas flow and/or longitudinal electric field, for example, created by segmented electrodes.[56,57] Hence, HODIMS could utilize any electrode geometry used for FAIMS, including planar, cylindrical, spherical, and their combinations.[10]

With a planar gap, any voltage waveform produces an electric field that is spatially homogeneous, except for fringe effects. The field becomes inhomogeneous in a curved gap, increasing toward the surface of higher curvature. In cylindrical and spherical FAIMS geometries, this causes focusing that keeps ions near the gap median (counteracting diffusion and Coulomb repulsion),[46,49] which greatly improves sensitivity and permits ion trapping at high pressures.[58,59] This effect would become stronger with increasing n because the dependence of E_C on E_D gets steeper, as follows from eqs 11, 16, 19, and 21. Therefore, HODIMS could also be performed in cylindrical geometries where ion focusing is critical, and enables the operation of atmospheric-pressure ion traps analogous to *t*-FAIMS.[58,59] In fact, the saturation ion currents of HODIMS analyzers and charge capacities of *t*-HODIMS traps may

TABLE 1: Characteristic Parameters of the Optimum Asymmetric Waveforms for FAIMS and Higher-Order Differential IMS up to the 5th Order

	$\Delta E/E_D$	$\Delta E_{tot}/E_D$	C_E
FAIMS	1.5	3	0.333
HODIMS, $n = 3$	1.81	3.62	0.324
HODIMS, $n = 4$	1.22−1.90	3.80−5.49	0.257−0.321
HODIMS, $n = 5$	1.27−1.94	3.88−6.42	0.209−0.320

significantly exceed those of FAIMS or *t*-FAIMS,[46,47] because of more effective ion focusing at higher *n*.

Choice of Asymmetric Waveform. As derived above, for $n \geq 4$ some of the optimum $E(t)$ produce ion trajectories with different Δr. A smaller Δr allows[47] a narrower analytical gap (in any geometry) and thus proportionately lower voltages for the same $E(t)$. The electrical engineering task is always simplified by minimizing rf voltages; hence, in general $E(t)$ that yield minimum Δr are best, that is, the waveforms (a, b) for $n = 4$ ($C_E \cong 0.257$, Figure 3) and (b, e, f, h) for $n = 5$ ($C_E \cong 0.209$, Figure 4). Other hardware considerations, such as finite switching speed, may favor $E(t)$ with smallest change between any consecutive voltage settings (ΔE). The optimum $E(t)$ forms have defined ΔE for $n = 2$ and 3, but not for higher *n*. For $n = 4$ (Figure 3), waveforms (e, f) involve $\Delta E \cong 1.22E_D$ versus $\cong 1.90\ E_D$ for (a − d). For $n = 5$ (Figure 4), the lowest $\Delta E \cong 1.27E_D$ is for (l) versus $\cong 1.50\ E_D$ (c), $\cong 1.73\ E_D$ (a, d, e, g), and $\cong 1.94\ E_D$ (b, f, h − k). However, for either $n = 4$ or $n = 5$, none of the ideal $E(t)$ that minimize Δr has the lowest ΔE and vice versa. Reducing the cumulative voltage change, ΔE_{tot}, per period (and thus the average electrical current in the system) may also be important, for example, because of power consumption or heat dissipation limitations. The waveforms for $n \geq 4$ have significantly different ΔE_{tot} values: $\cong 3.80E_D$ (c − f) and $\cong 5.49E_D$ (a, b) for $n = 4$; and $\cong 3.88E_D$ (c, g, j, l), $\cong 5.07E_D$ (d, i), $\cong 5.23E_D$ (a, k), and $\cong 6.42E_D$ (b, e, f, h) for $n = 5$. As seen here, the lowest ΔE_{tot} is compatible with the lowest ΔE, pointing to options (e, f) for $n = 4$ and option (l) for $n = 5$ as perhaps the most practical for engineering. However, minimization of ΔE_{tot} is inconsistent with that of Δr, and the latter may be preferable. The overall magnitudes of ΔE and ΔE_{tot} for HODIMS of 3rd to 5th orders are close to those for FAIMS (Table 1), indicating broadly similar implementation issues.

Each $E(t)$ may have two polarities. In FAIMS, these are interchangeable for planar geometries but not for curved ones where the ion focusing depends on polarity.[3,49] The proper polarity is set by the combination of the sign of ion charge and the sign of *a*, creating four modes:[3,49] P1, P2, N1, and N2. This would also happen in HODIMS for any *n*, except that the polarity would depend on the sign of another higher-order coefficient for the chosen *n*. FAIMS measurements[31] indicate that both $b > 0$ and $b < 0$ are possible, and the same should apply for *c*, *d*, ... Hence, all four FAIMS modes would likely be mirrored in HODIMS of any order. Signs of the different coefficients in eq 3 are generally mutually independent (e.g., ions with positive *a* may have[31] either positive or negative *b*, and ions with negative *b* may have[33] either positive or negative *a*); hence, changing *n* may necessitate switching the waveform polarity.

In practical FAIMS analyzers, the ideal $E(t)$ of eq 9 is approximated by either a bisinusoidal (a sum of two harmonics)[31,46,47,53] or a clipped displaced sinusoidal.[47,60] Substitution of these waveforms for the rectangular $E(t)$ in FAIMS sacrifices some resolution and/or sensitivity,[47] but simplifies the design. Similarly, HODIMS could use $E(t)$ forms that are fundamentally sub-optimal, but easier or less expensive to implement.

Intensity of Electric Field and Separation Power. In principle, a differential IMS effect (for any *n*) exists at any *E*. However, the FAIMS resolution depends[45] on $\langle v \rangle$, which scales as E_D^3 (eq 10), and the separation becomes useful[31,33,49,54,61] at $E_D/N \approx 40-50$ Td, with optimum performance achieved at ∼65−80 Td. By the nature of eq 3, the value of E/N at which a term exceeds a given threshold tends to increase for each subsequent term. Thus, higher separation orders require greater E/N, and a steeper dependence of $\langle v \rangle$ on E_D at higher *n* means an increasingly abrupt emergence of a significant effect.

The strongest field allowable in any gas is limited by electrical breakdown, with the point of onset depending on the gas properties (identity and *N*), the gap width (*g*), and, to a lesser extent, electrode geometry.[62] In existing FAIMS systems (including the commercial Selectra and DMS), E_{BR}/N (for N_2 or air at STP conditions) ranges[62] from ∼160 Td for $g = 2$ mm to ∼220 Td for $g = 0.5$ mm. The increase in required E_D at higher *n* will obviously preclude useful operation beyond a certain *n*. So, a key concern is whether the HODIMS effect would be large enough for practical separations at realistic electric field intensities.

The E_D needed for HODIMS would depend on the magnitude of coefficient in eq 3 with the chosen *n*. Unfortunately, the information about those values is scarce for $n = 3$ and barely existent for $n > 3$. About the only sizable compilation of *b* values comes from FAIMS data for protonated and deprotonated ions of 17 amino acids in air,[31] where *b* (below in 10^{-10} Td^{-4}) ranges from −5.95 to 0.79 with $\langle |b| \rangle = 1.47$ and median $|b| = 1.34$. As already stated, in the same set, $a = 1.27-17.4$, with $\langle a \rangle = 6.78$ and median $a = 6.00$. The similarity of means and medians in both sets suggests a representative selection of *a* and *b*. These data allow estimating E_D/N that, for $n = 3$, would provide E_C (and thus the resolution) comparable to those in FAIMS at typical E_D (Figure 5a). In FAIMS using the ideal waveform, a hypothetical ion with mean {*a*; *b*} would have $E_C \approx 100-180$ V/cm at $E_D/N = 65-80$ Td. In 3rd order separations, E_C would reach the same magnitude at $E_D/N \approx 130-150$ Td, which is below the electrical breakdown threshold even in the worst case of $g = 2$ mm. The $|b|/|a|$ ratio for many ions in the set exceeds the mean of 22×10^{-6} Td^{-2}, and a comparable E_C would be obtained at lower E_D. For example, H^+lysine with[31] $a = 3.83$; $b = -2.51$ ($|b|/|a| = 66 \times 10^{-6}$ Td^{-2}) has a lower $E_C \approx 45-60$ V/cm at $E_D/N = 65-80$ Td in FAIMS. Achieving equal E_C in 3rd order HODIMS would only require $E_D/N \approx 100-110$ Td (Figure 5a), a field already employed in some FAIMS studies.[33,54] Recalling that FAIMS becomes useful at $E_D/N \approx 40-50$ Td, one may estimate the fields needed for similar HODIMS performance as ∼100−115 Td for an "average" amino acid and ∼90−105 Td for H^+lysine (Figure 5a). Some ions have low $|b|$ that would not yield a significant E_C at any achievable E_D/N. However, this situation is not specific to HODIMS but inherent in differential IMS, for example, FAIMS for ions with[33,54] $a \approx 0$. We appreciate that *a* and *b* in the above set are for $E/N \leq 65$ Td and should not be extrapolated to higher fields. The aim here is not to predict separation parameters for particular species, but to gauge the electric field strength that may be useful for higher-order IMS in general.

Similar estimates could be derived from the other three published (less extensive) sets of *b*, also deduced from FAIMS measurements in air.[33,54,55] The $\{\langle |a| \rangle; \langle |b| \rangle\}$ values of those sets are {16.0; 9.26} for 8 protonated ketones from acetone to decanone[33] ($m = 59-157$ Da), {3.94; 8.18} for their dimers,[33] {2.57; 1.06} for 10 protonated organophosphorus compounds

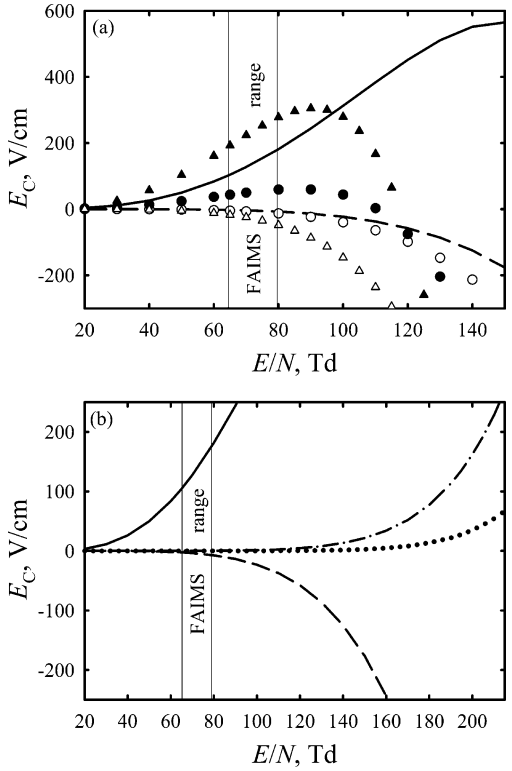

Figure 5. Compensation field for representative ions in FAIMS and HODIMS computed as a function of dispersion field. Lines in both panels are for a hypothetical "average" amino acid described in the text, for separation orders of $n = 2$ in FAIMS (solid), $n = 3$ (dashed), $n = 4$ (dash−dot), and $n = 5$ (dotted). In (a), filled symbols are for FAIMS and empty ones are for 3rd order HODIMS: circles for H^+-lysine and triangles for an "average" ketone.

($m = 125-267$ Da),[54] {0.58; 0.73} for 7 of their dimers,[54] and {9.61; 7.18} for 9 cations of organic volatiles with $m = 78-169$ Da (benzene, *o*-toluidine, dimethyl methylphosphonate, and six aromatic amines).[55] Thus, typical $|b|$ for organophosphorus ions are close to those for amino acids, and those for the other two sets are nearly an order of magnitude higher. Hence, the 3rd order HODIMS for many smaller organic ions would already become operational at $E_D/N \approx 70-80$ Td and as effective as standard FAIMS at ∼100−115 Td (Figure 5a).

Feasibility of HODIMS with $n > 3$. Little is known about the values of *c*, *d*, ... that control HODIMS for $n \geq 4$. The coefficients *c* have been measured only for the above-mentioned set of nine organic ions (using FAIMS at very high E/N).[55] The resulting values (at $T = 20$ °C, in 10^{-14} Td^{-6}) are 1.29−4.76 with $\langle|c|\rangle = 2.86$, which allows projecting typical separation parameters for 4th order HODIMS. In this scenario, a useful operation could be achieved at $E_D/N \approx 110-125$ Td, which is just above the highest $E_D/N \approx 110$ Td employed in FAIMS[33,54] and well below the breakdown threshold for any gap width.

General magnitudes of *c*, *d*, ... could be estimated considering that, in Taylor expansions describing physical phenomena such as eq 3, the ratios of absolute coefficients with consecutive terms often lie within an order of magnitude. Indeed, for the above organic ion set,[55] those ratios (in 10^{-6} Td^{-2}) are: $\langle|c|\rangle/\langle|b|\rangle = 40$, $\langle|b|\rangle/\langle|a|\rangle = 75$, and $\langle|a|\rangle = 9.6$. Similarly, $\langle|b|\rangle/\langle|a|\rangle = 58$ and $\langle|a|\rangle = 16$ for the ketones,[33] and $\langle|b|\rangle/\langle|a|\rangle = 22$ and $\langle|a|\rangle = 6.8$ for the amino acids.[31] Assuming

$$\langle|d|\rangle/\langle|c|\rangle = \langle|c|\rangle/\langle|b|\rangle = \langle|b|\rangle/\langle|a|\rangle \qquad (22)$$

yields $\langle|d|\rangle = 1.1-2.1$ (in 10^{-18} Td^{-8}) for nine organic ions,[55] $\langle|c|\rangle = 5.4$ and $\langle|d|\rangle = 3.1$ for ketones, and $\langle|c|\rangle = 0.32$ and $\langle|d|\rangle = 0.069$ for amino acids. The values for ketones would allow useful HODIMS operation at even lower E_D/N than those for the organic ion set:[55] ∼100−115 Td for $n = 4$ and 125−135 Td for $n = 5$, that is, not enough for breakdown under any conditions. On the other hand, separations for amino acids would require $E_D/N \approx 150-170$ Td ($n = 4$) and ∼190−210 Td ($n = 5$). These values are slightly below the realistic E_{BR}/N range for $n = 4$ but within it for $n = 5$, potentially a significant complication. While the estimates derived from eq 22 are quite crude, they show that 4th and even 5th order HODIMS should be achievable at realistic electric field intensities, at least for many ions.

All comparisons above have been made versus ideal FAIMS with a rectangular $E(t)$ that is more effective[47] than actual sinusoid-based waveforms by ∼50%. Thus, HODIMS with the ideal $E(t)$ considered here would be similarly more effective by ∼50% if benchmarked against conventional FAIMS. Of course, real HODIMS waveforms would not be optimum either.

HODIMS in Electrically Insulating Media. Like FAIMS, higher-order separations could use gases other than N_2 or air, some of which are significantly more resistant to electrical breakdown. For example, a gap of 0.5−2 mm filled with SF_6 (a common gas-phase insulator in industry) supports $E/N \approx 380-410$ Td, and yet higher E/N values are accessible using electronegative gases based on halogenated carbons.[62] While FAIMS in SF_6 has been reported,[30] the values of *b*, *c*, *d*... are not known for any ion. However, values of *a* for several representative ions in SF_6 are close[30] to those in N_2 and O_2, and there is no reason for other coefficients to be abnormally low. Accordingly, the ability to raise E_D/N to ∼400 Td should allow useful separations up to $n = 5$, and perhaps for yet higher orders. When operation in pure insulating gases is impractical, even a small admixture of those to the buffer (such as air or N_2) raises the breakdown threshold disproportionately to the fraction of insulating gas.[62] For example, the threshold for 90:10 N_2/SF_6 is ∼150% that for pure N_2.

Gap Width and Waveform Frequency. The optimum gap width in differential IMS is determined by Δr for ions of interest: *g* less than or close to Δr would cause an indiscriminate rapid elimination of ions, whereas too wide a gap would pass significantly unbalanced ions resulting in poor separation quality.[47] By eq 17, Δr is proportional to C_E and E_D, and both parameters differ from those in FAIMS and depend on *n* as discussed above. However, the decrease of optimum C_E and increase of required E_D with increasing *n* partly offset each other. For example, with the lowest C_E possible for a given *n* (Table 1) and reasonable E_D/N of 80, 130, 160, and 200 Td for $n = 2-5$, the respective $C_E E_D/N$ quantities are 26.7, 42.1, 41.1, and 41.8 Td. Thus, HODIMS for all *n* considered would involve approximately equal Δr that differ from typical FAIMS values by a factor of only ∼1.5, which indicates that separations of all higher orders could be implemented using one gap width. Other factors being equal, the gap would ideally be somewhat wider than for FAIMS, with the waveform voltage scaled to establish the same E_D. Alternatively, one could increase the waveform frequency in proportion to $C_E E_D/N$ to produce constant Δr by eq 17. Regardless, these estimates suggest that HODIMS could use existing FAIMS mechanical hardware, allowing a rapid switching between all $n \geq 2$ orders on the software level by changing only the $E(t)$ profile and possibly adjusting the amplitude and/or frequency.

Potential Utility of Higher-Order Separations

The preceding discussion has examined the fundamental and practical feasibility of higher-order differential IMS. The

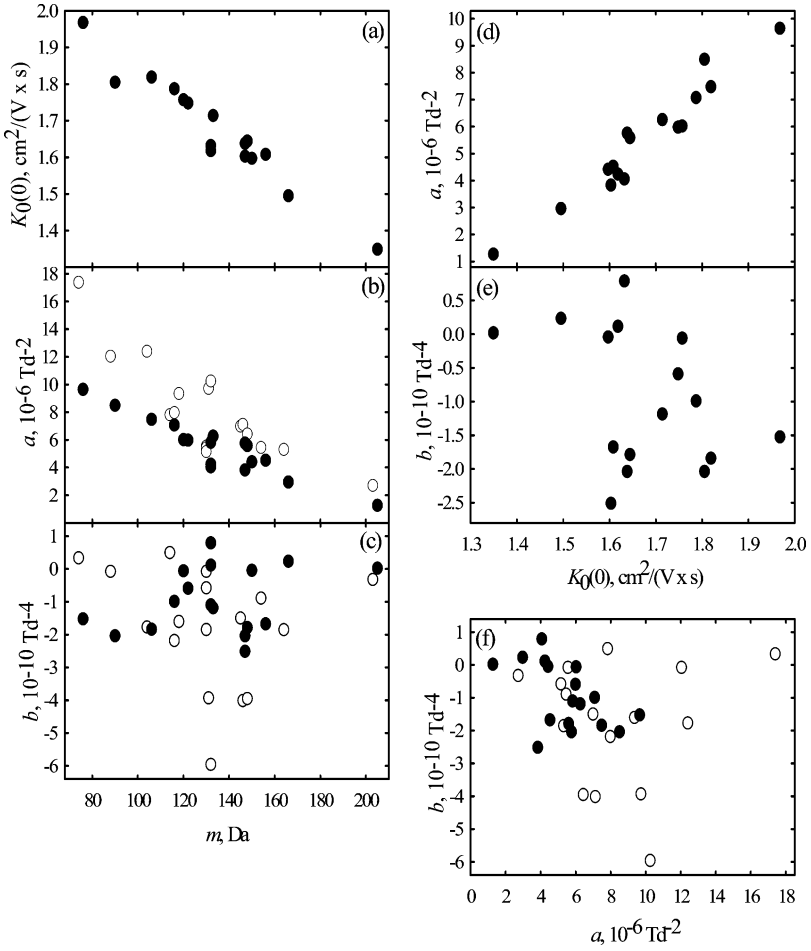

Figure 6. Pairwise correlations between ion mass, low-field mobility, and coefficients *a* and *b* for amino acid cations (●) and anions (○). Values are from IMS[73] and FAIMS[31] measurements (in N_2 gas). Slightly different $K_0(0)$ values were reported (Beegle, L. W.; Kanik, I.; Matz, L.; Hill, H. H., Jr. *Anal. Chem.* **2001**, *73*, 3028), but the effect on r^2 is negligible. Absolute mobilities for anions have not been measured.

remaining question is whether HODIMS would be of analytical utility, that is, what advantages and new capabilities would be provided?

Orthogonality to MS. As mentioned in the introduction, FAIMS and MS tend to be more orthogonal than IMS and MS. There also is a significant orthogonality between FAIMS and IMS dimensions,[63,64] which enables 2-D separations by FAIMS/IMS coupling.[64] However, FAIMS is still substantially correlated to MS. For example, in FAIMS in N_2 or air buffer, small ions with masses up to several hundred Da (including monatomics,[30] all amino acid ions,[31] and other simple organic ions[33,54]) are "A-type"[49] (i.e., have a positive *a*), while large ions (including all peptides[24,53,63,64]) are "C-type"[49] (i.e., have a negative *a*). The inverse correlation between *a* and *m* is also found within many homologous series, for example, for the previously introduced organophosphorus compounds,[54] ketones,[33] and aromatic amines,[55] halogenate anions,[65] and amino acids (below).[31] Classification of ions by types depends on the gas; an "A" ion in one buffer (e.g., Cs^+ in N_2 or O_2)[30,66] may become "C" in another (e.g., Cs^+ in He).[67] Nonetheless, the trend of *a* decreasing with increasing ion mass remains, in agreement with basic ion−molecule collision dynamics.[30]

A priori, the orthogonality between HODIMS and MS should increase with increasing *n* for the same reason FAIMS is generally more orthogonal to MS than is IMS. Measurements for amino acid cations and anions support this conjecture (Figure 6). All ions in these experiments are singly charged, so $m/z = \pm m$. Absolute mobilities are tightly related to mass, with the r^2 of linear correlation equal to 0.93 (Figure 6a). The r^2 of correlation between coefficient *a* and *m* is lower, but still large: 0.87 for 1+ and 0.71 for 1− ions (Figure 6b). To the contrary, the values of *b* are independent of *m* (Figure 6c, $r^2 = 0.09$ for 1+ and 0.04 for 1−). In the absence of a linear correlation, probing for higher-order statistical correlations is important. The data in Figure 6c do not exhibit such either; for example, the quadratic (r_2) and cubic (r_3) correlations are $r_2^2 = 0.09$, $r_3^2 = 0.15$ for 1+ and $r_2^2 = 0.27$, $r_3^2 = 0.28$ for 1−. So, unlike FAIMS or IMS, 3rd order separations of amino acids would be orthogonal to MS. In less favorable cases (e.g., for the sets of ketones,[33] organophosphorus compounds,[54] and organic volatiles[55]), HODIMS with $n = 3$ and MS remain correlated, but generally weaker than FAIMS and MS. For example, for the above set[55] of nine organic ions, r^2 is 0.84 and 0.58 for the plots of *a* versus *m* (Figure 7a) and *b* versus *m* (Figure 7b), respectively.

From the first principles, HODIMS separations for $n \geq 4$ should be yet more orthogonal to MS than those for $n = 3$. This surmise is supported by the coefficients *c* measured for the organic ion set.[55] The r^2 of correlation between *c* and *m* (Figure 7c) is 0.00, indicating a perfect orthogonality of the 4th order HODIMS to MS.

Both IMS/MS[37−42,68] and FAIMS/MS[69−72] are frequently employed for analyses of isomeric/isobaric ions; however, the correlation between two dimensions is an ubiquitous challenge. More generally, this results in relatively low 2-D peak capacities that impede analyses of complex mixtures. A high orthogonality between HODIMS and MS could make HODIMS/MS preferable to IMS/MS or FAIMS/MS, even at inferior resolution. For

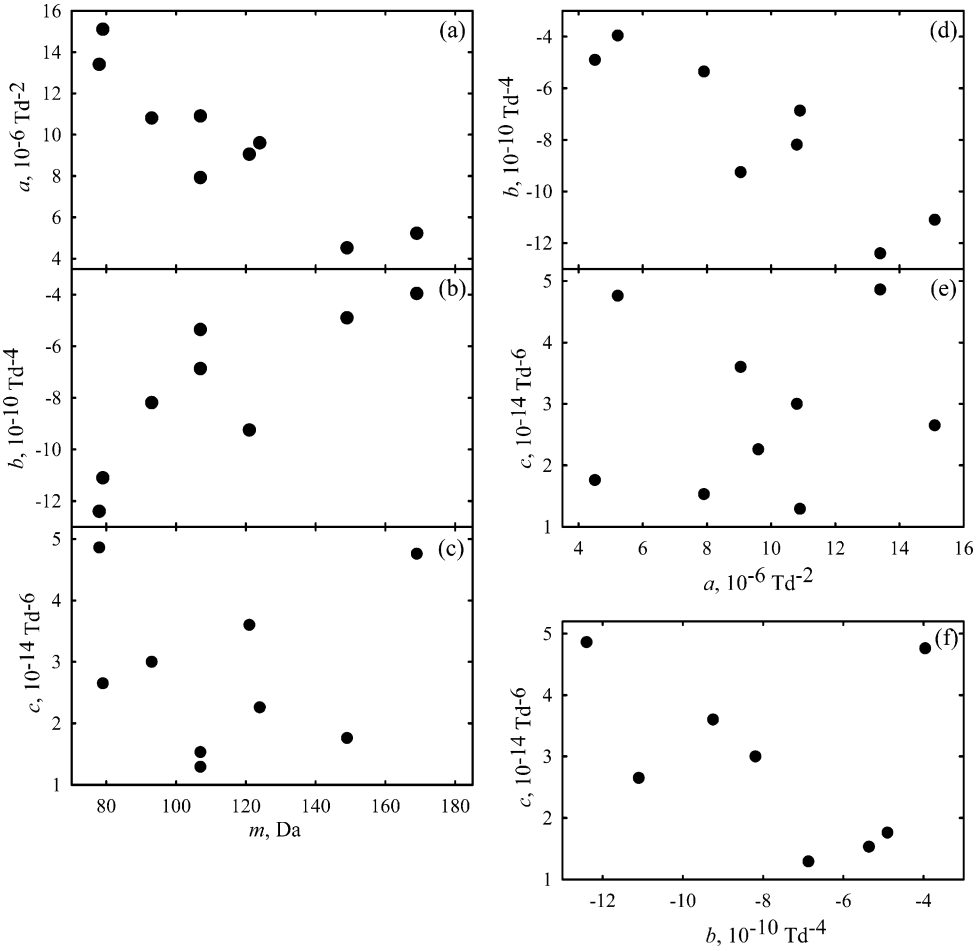

Figure 7. Pairwise correlations between ion mass and coefficients *a*, *b*, and *c* for nine small organic cations, from FAIMS measurements[55] (in air at 20 °C).

example, the mobilities of H^+leucine and H^+isoleucine in N_2 differ by 1% (1.618 and 1.632 $cm^2/(V\cdot s)$, respectively),[73] which barely allows distinguishing these isomers in IMS.[5] The difference between coefficients *a* (respectively, 4.24 and 4.06) is greater[31] at 4%, but again is just sufficient for FAIMS separation.[46,47] Similarly, for anions, *a* for (leucine − H)$^-$ and (isoleucine − H)$^-$ differs[31] by 5% (respectively, 5.43 and 5.15), which is just enough for FAIMS analyses.[69] In comparison, the values of *b* differ[31] by ∼560% (0.12 vs 0.79) for cations and ∼220% (−1.85 vs −0.58) for anions. This magnitude of difference should allow a complete separation even with a limited resolution. More accurately, the difference between separation parameters of two species should be compared to the separation space width. For cations, that width equals 8.38 in the *a* dimension and 3.30 in the *b* dimension.[31] Hence, the peak capacities needed to distinguish H^+leucine from H^+-isoleucine are 8.38/(4.24−4.06) = 47 in FAIMS and 3.30/(0.79−0.12) = 4.9 in 3rd order HODIMS. Similarly, for anions, the separation space width is[31] 14.7 for *a* and 6.45 for *b*, and the peak capacities needed are 52 in FAIMS, but only 4.8 in HODIMS for $n = 3$. In other words, HODIMS could possibly provide a peak capacity 10 times higher than FAIMS at equal resolution or equal to FAIMS at ∼1/10 resolution. This means that HODIMS could potentially operate at roughly one-half the electric field projected in the preceding section based on FAIMS resolution benchmarks, which would place the required E_D/N for all $n \leq 5$ in the standard FAIMS range of <110 Td.

New Multidimensional Gas-Phase Separations. In addition to orthogonality to MS, higher-order separations would also be substantially independent of IMS and FAIMS. For example, for the amino acid set,[31] HODIMS with $n = 3$ would be orthogonal to IMS with $r^2 = 0.15$, $r_2^2 = 0.16$, and $r_3^2 = 0.16$ (Figure 6e), while FAIMS and IMS are correlated as tightly as IMS and MS (Figure 6d, $r^2 = 0.93$). Moreover, 3rd order HODIMS would be independent of FAIMS with $r^2 = 0.25$, $r_2^2 = 0.25$, and $r_3^2 = 0.26$ for 1+ and $r^2 = 0.00$, $r_2^2 = 0.24$, and $r_3^2 = 0.24$ for 1− (Figure 6f). HODIMS then could be usefully coupled to IMS and/or FAIMS to enable 2-D and even 3-D gas-phase separations, either with or without MS analyses. HODIMS could also be interfaced with condensed-phase separations such as reverse-phase and/or strong cation exchange liquid chromatography in front of an ion source, as presently practiced for IMS[6,15,16] and FAIMS.[24]

A priori, the orthogonality of HODIMS to IMS and FAIMS (like that to MS) should increase for higher *n*. Indeed, for the organic ion set,[55] *c* and *a* are fully independent (Figure 7e, $r^2 = 0.01$), while *b* and *a* are moderately correlated (Figure 7d, $r^2 = 0.58$). Finally, lack of correlation between *b* and *c* (Figure 7f, $r^2 = 0.14$) suggests orthogonality between HODIMS separation of various orders. Thus, separations in further dimensions could, in principle, be achieved by stacking HODIMS operated at different *n*. In particular, multidimensional methods involving IMS of different orders without MS is a promising route to high specificity in field analyses where ruggedness, power consumption, weight, and/or footprint are major concerns.

The Effect of Temperature. Each term of eq 3 is a functional of ion−molecule collision integrals that depend on the gas temperature.[29] Therefore, as is well-known in IMS,[38,74,75] the separation parameters in ion mobility methods of any order are

temperature-dependent. The effect generally increases for higher n, where small changes of mobility as a function of temperature are magnified by differential measurement. For example, for the benzene cation in air,[55] heating from 10 to 40 °C changes a by 7% (from 12.9 to 13.8), b by ~70% (from −9.36 to −16.2), and c by >300% (from 2.22 to 9.13). For the *o*-toluidine cation,[55] a changes by 1% (from 7.94 to 8.00), b by 10% (from −5.38 to −5.93), and c by 12% (from 1.61 to 1.44). These data further suggest that the effect of temperature on HODIMS separation parameters would vary from ion to ion a lot. This would enable modifying the separation properties to distinguish hard-to-resolve species using fine temperature control.

Directions for Future Work

We have introduced the concept of higher-order mobility separations and addressed the key issues that determine their feasibility and potential utility. Follow-up efforts will optimize the hardware design and operation for HODIMS implementation. First, we are extending the FAIMS molecular dynamics simulation[46,47,57] to waveforms involved in HODIMS. That would permit a comprehensive treatment of HODIMS separations (including an accurate modeling of resolution, ion transmission efficiency, and ion focusing and trapping) that would guide instrumental development and choice of experimental parameters. Second, successful realization of HODIMS would depend on approximating the ideal waveforms by superposed harmonics in a way that judiciously balances the operational efficiency and engineering complexity. Hence, optimizing the emulation of ideal $E(t)$ by harmonic functions will be a priority for simulations. Finally, non-Blanc effects that control and often strongly benefit FAIMS in heteromolecular gases[9] will also appear in higher-order separations. As is common for nonlinear phenomena, these effects could become more pronounced at higher separation orders. We will explore this matter using the established formalisms for FAIMS in gas mixtures.[9]

Conclusions

We have derived from physical fundamentals that ion mixtures could be fractionated on the basis of any term of power expansion for ion mobility in gases, allowing an infinite number of distinct separations. New differential mobility methods would distinguish ions by the coefficients with 3rd and higher terms of that expansion, analogously to FAIMS governed by the coefficient with 2nd term. In principle, methods of any order n are possible using periodic time-dependent electric fields that comprise at least n discrete segments, all with different field intensities. In this paradigm, known IMS and FAIMS are separations of 1st and 2nd order that require waveforms consisting of a single segment (i.e., a constant field) and two segments with "high" and "low" fields, respectively. The waveforms for separations of all n are optimized when the duration of the segment with the strongest field is one-half that of all others. The relative field intensities of all segments depend on n, and the procedure to calculate them for any n is presented and exemplified for $n \leq 5$. Choice of the order of segments within the period is also important and would be determined by balancing competing engineering considerations.

Higher-order differential IMS (HODIMS) could be implemented using electrode sets similar to those in FAIMS and perhaps even the existing FAIMS mechanical hardware, which would allow switching or gradually transitioning between separation orders in the same analyzer. In particular, HODIMS could employ known planar, cylindrical, and spherical FAIMS geometries, and, with proper waveform polarity, would exhibit ion focusing in the latter two. This focusing would allow high-pressure ion trapping analogous to that in spherical FAIMS. The ion focusing in HODIMS could be superior to that in FAIMS, potentially enabling analyzers, guides, and traps with charge capacities above those of FAIMS analogues. The electric field strength needed for differential IMS separations would generally increase with increasing n, for $n = 3-5$ exceeding typical FAIMS values by a factor of ~1.5−2. Such fields could be established without electrical breakdown in air or N_2, and some other gases (e.g., SF_6 and its mixtures) support much higher fields that might allow HODIMS even for $n > 5$. The waveforms for HODIMS would have somewhat higher amplitudes (and perhaps frequencies) than those for FAIMS, but should be achievable using similar engineering approaches.

High-field ion mobility data for amino acid and other organic ions suggest that HODIMS of different orders would be largely independent of each other and of FAIMS, IMS, and MS, with orthogonality increasing at higher separation orders. Hence, the HODIMS/MS combination could substantially outperform IMS/MS and FAIMS/MS in terms of 2-D peak capacity, even with a lower resolution. HODIMS separation parameters are anticipated to exhibit strong temperature dependence, allowing fine control of analyses by adjustment of gas temperature. Multidimensional gas-phase separations could be achieved by coupling ion mobility methods of different orders (including conventional IMS and FAIMS), with or without MS.

Acknowledgment. We thank Dr. Keqi Tang and Gordon Anderson at Pacific Northwest National Laboratory (PNNL) for many insightful discussions of differential IMS and their technical implementation. This work was supported by the NIH National Center for Research Resources (RR 18522). PNNL is a multi-program national laboratory operated by the Battelle Memorial Institute for the U.S. Department of Energy through Contract DE-ACO5-76RLO1830.

References and Notes

(1) von Helden, G.; Wyttenbach, T.; Bowers, M. T. *Int. J. Mass Spectrom. Ion Processes* **1995**, *146*, 349.
(2) Clemmer, D. E.; Hudgins, R. R.; Jarrold, M. F. *J. Am. Chem. Soc.* **1995**, *117*, 10141.
(3) Purves, R. W.; Guevremont, R. *Anal. Chem.* **1999**, *71*, 2346.
(4) Hoaglund, C. S.; Valentine, S. J.; Sporleder, C. R.; Reilly, J. P.; Clemmer, D. E. *Anal. Chem.* **1998**, *70*, 2236.
(5) Asbury, G. R.; Hill, H. H. *J. Microcolumn. Sep.* **2000**, *12*, 172.
(6) Srebalus Barnes, C. A.; Hilderbrand, A. E.; Valentine, S. J.; Clemmer, D. E. *Anal. Chem.* **2002**, *74*, 26.
(7) Koeniger, S. L.; Valentine, S. J.; Myung, S.; Plasencia, M.; Lee, Y. L.; Clemmer, D. E. *J. Proteome Res.* **2005**, *4*, 25.
(8) Tang, K.; Shvartsburg, A. A.; Lee, H. N.; Prior, D. C.; Buschbach, M. A.; Li, F.; Tolmachev, A. V.; Anderson, G. A.; Smith, R. D. *Anal. Chem.* **2005**, *77*, 3330.
(9) Shvartsburg, A. A.; Tang, K.; Smith, R. D. *Anal. Chem.* **2004**, *76*, 7366.
(10) Guevremont, R.; Thekkadath, G.; Hilton, C. K. *J. Am. Soc. Mass Spectrom.* **2005**, *16*, 948.
(11) Thalassinos, K.; Slade, S. E.; Jennings, K. R.; Scrivens, J. H.; Giles, K.; Wildgoose, J.; Hoyes, J.; Bateman, R. H.; Bowers, M. T. *Int. J. Mass Spectrom.* **2004**, *236*, 55.
(12) Steiner, W. E.; Clowers, B. H.; Fuhrer, K.; Gonin, M.; Matz, L. M.; Siems, W. F.; Schultz, A. J.; Hill, H. H. *Rapid Commun. Mass Spectrom.* **2001**, *15*, 2221.
(13) Guevremont, R. *J. Chromatogr., A* **2004**, *1058*, 3.
(14) Eiceman, G. A.; Krylov, E. V.; Krylova, N. S.; Nazarov, E. G.; Miller, R. A. *Anal. Chem.* **2004**, *76*, 4937.
(15) Moon, M. H.; Myung, S.; Plasencia, M.; Hilderbrand, A. E.; Clemmer, D. E. *J. Proteome Res.* **2003**, *2*, 589.
(16) Myung, S.; Lee, Y. J.; Moon, M. H.; Taraszka, J.; Sowell, R.; Koeniger, S.; Hilderbrand, A. E.; Valentine, S. J.; Cherbas, L.; Cherbas, P.; Kaufmann, T. C.; Miller, D. F.; Mechref, Y.; Novotny, M. V.; Ewing, M. A.; Sporleder, C. R.; Clemmer, D. E. *Anal. Chem.* **2003**, *75*, 5137.

(17) Woods, A. S.; Ugarov, M.; Egan, T.; Koomen, J.; Gillig, K. J.; Fuhrer, K.; Gonin, M.; Schultz, J. A. *Anal. Chem*. **2004**, *76*, 2187.
(18) Ruotolo, B. T.; Gillig, K. J.; Woods, A. S.; Egan, T. F.; Ugarov, M. V.; Schultz, J. A.; Russell, D. H. *Anal. Chem.* **2004**, *76*, 6727.
(19) Jackson, S. N.; Wang, H. Y. J.; Woods, A. S. *J. Am. Soc. Mass Spectrom*. **2005**, *16*, 133.
(20) Tempez, A.; Ugarov, M.; Egan, T.; Schultz, J. A.; Novikov, A.; Della-Negra, S.; Lebeyec, Y.; Pautrat, M.; Caroff, M.; Smentkowski, V. S.; Wang, H.-Y. J.; Jackson, S. N.; Woods, A. S. *J. Proteome Res*. **2005**, *4*, 540.
(21) McLean, J. A.; Ruotolo, B. T.; Gillig, K. J.; Russell, D. H. *Int. J. Mass Spectrom*. **2005**, *240*, 301.
(22) McCooeye, M. A.; Zoltan, M.; Ells, B.; Barnett, D. A.; Purves, R. W.; Guevremont, R. *Anal. Chem.* **2002**, *74*, 3071.
(23) Cui, M.; Ding, L.; Mester, Z. *Anal. Chem.* **2003**, *75*, 5847.
(24) Venne, K.; Bonneil, E.; Eng, K.; Thibault, P. *Anal. Chem.* **2005**, ***77***, 2176.
(25) Carr, T. W. *Anal. Chem*. **1979**, *51*, 705.
(26) Lubman, D. M.; Kronick, M. N. *Anal. Chem.* **1982**, *54*, 1546.
(27) Hill, H. H.; Siems, W. F.; St. Louis, R. H.; McMinn, D. G. *Anal. Chem.* **1990**, *62*, A1201.
(28) Shumate, C. B.; Hill, H. H. *Anal. Chem.* **1989**, *61*, 601.
(29) Mason, E. A.; McDaniel, E. W. *Transport Properties of Ions in Gases*; Wiley: New York, 1988.
(30) Barnett, D. A.; Ells, B.; Guevremont, R.; Purves, R. W.; Viehland, L. A. *J. Am. Soc. Mass Spectrom.* **2000**, *11*, 1125.
(31) Guevremont, R.; Purves, R. W.; Barnett, D. A.; Viehland, L. A. *J. Chem. Phys*. **2001**, *114*, 10270.
(32) Viehland, L. A.; Guevremont, R.; Purves, R. W.; Barnett, D. A. *Int. J. Mass Spectrom.* **2000**, *197*, 123.
(33) Krylov, E.; Nazarov, E. G.; Miller, R. A.; Tadjikov, B.; Eiceman, G. A. *J. Phys. Chem. A* **2002**, *106*, 5437.
(34) Thomson, G. M.; Schummers, J. H.; James, D. R.; Graham, E.; Gatland, I. R.; Flannery, M. R.; McDaniel, E. W. *J. Chem. Phys.* **1973**, *58*, 2402.
(35) Viggiano, A. A.; Morris, R. A.; Mason, E. A. *J. Chem. Phys.* **1993**, *98*, 6483.
(36) Viehland, L. A.; Lozeille, J.; Soldán, P.; Lee, E. P. F.; Wright, T. G. *J. Chem. Phys*. **2003**, *119*, 3729.
(37) Bowers, M. T.; Kemper, P. R.; von Helden, G.; van Koppen, P. A. M. *Science* **1993**, *260*, 1446.
(38) Shvartsburg, A. A.; Schatz, G. C.; Jarrold, M. F. *J. Chem. Phys*. **1998**, *108*, 2416.
(39) Shvartsburg, A. A.; Hudgins, R. R.; Dugourd, Ph.; Gutierrez, R.; Frauenheim, T.; Jarrold, M. F. *Phys. Rev. Lett*. **2000**, *84*, 2421.
(40) Ho, K. M.; Shvartsburg, A. A.; Pan, B.; Lu, Z. Y.; Wang, C. Z.; Wacker, J. G.; Fye, J. L.; Jarrold, M. F. *Nature* **1998**, *392*, 582.
(41) Shvartsburg, A. A.; Jarrold, M. F. *Phys. Rev. A* **1999**, *60*, 1235.
(42) Shvartsburg, A. A.; Hudgins, R. R.; Dugourd, P.; Jarrold, M. F. *Chem. Soc. Rev.* **2001**, *30*, 26.
(43) Ruotolo, B. T.; Gillig, K. J.; Stone, E. G.; Russell, D. H. *J. Chromatogr., B* **2002**, *782*, 385.
(44) Shvartsburg, A. A.; Siu, K. W. M.; Clemmer, D. E. *J. Am. Soc. Mass Spectrom.* **2001**, *12*, 885.
(45) Buryakov, I. A.; Krylov, E. V.; Soldatov, V. P. USSR Inventor's Certificate # 1,337,934, 1987.
(46) Shvartsburg, A. A.; Tang, K.; Smith, R. D. *J. Am. Soc. Mass Spectrom.* **2004**, *15*, 1487.
(47) Shvartsburg, A. A.; Tang, K.; Smith, R. D. *J. Am. Soc. Mass Spectrom.* **2005**, *16*, 2.
(48) Spangler, G. E.; Miller, R. A. *Int. J. Mass Spectrom.* **2002**, *214*, 95.
(49) Purves, R. W.; Guevremont, R.; Day, S.; Pipich, C. W.; Matyjaszczyk, M. S. *Rev. Sci. Instrum*. **1998**, *69*, 4094.
(50) Miller, R. A.; Nazarov, E. G.; Eiceman, G. A.; King, T. A. *Sens. Actuators, A* **2001**, *91*, 301.
(51) Buryakov, I. A.; Krylov, E. V.; Soldatov, V. P. USSR Inventor's Certificate # 1,485,808, 1989.
(52) Guevremont, R.; Purves, R.; Barnett, D. U.S. Patent # 6,713,758, 2004.
(53) Barnett, D. A.; Ells, B.; Guevremont, R.; Purves, R. W. *J. Am. Soc. Mass Spectrom.* **2002**, *13*, 1282.
(54) Krylova, N.; Krylov, E.; Eiceman, G. A.; Stone, J. A. *J. Phys. Chem. A* **2003**, *107*, 3648.
(55) Buryakov, I. A. *Tech. Phys*. **2004**, *49*, 967.
(56) Miller, R. A.; Zahn, M. U.S. Patent # 6,512,224, 2003.
(57) Shvartsburg, A. A.; Tang, K.; Smith, R. D. *J. Am. Soc. Mass Spectrom.* **2005**, *16*, 1447.
(58) Guevremont, R.; Purves, R. W.; Barnett, D. A.; Ding, L. *Int. J. Mass Spectrom.* **1999**, *193*, 45.
(59) Guevremont, R.; Ding, L.; Ells, B.; Barnett, D. A.; Purves, R. W. *J. Am. Soc. Mass Spectrom.* **2001**, *12*, 1320.
(60) Buryakov, I. A. *Talanta* **2003**, *61*, 369.
(61) Ells, B.; Barnett, D. A.; Froese, K.; Purves, R. W.; Hrudey, S.; Guevremont, R. *Anal. Chem.* **1999**, *71*, 4747.
(62) Meek, J. M., Craggs, J. D., Eds. *Electrical Breakdown of Gases*; Wiley: New York, 1978.
(63) Guevremont, R.; Barnett, D. A.; Purves, R. W.; Vandermey, J. *Anal. Chem*. **2000**, *72*, 4577.
(64) Tang, K.; Li, F.; Shvartsburg, A. A.; Strittmatter, E. F.; Smith, R. D. *Anal. Chem*. **2005**, *77*, 6381.
(65) Barnett, D. A.; Guevremont, R.; Purves, R. W. *Appl. Spectrosc*. **1999**, *53*, 1367.
(66) Thackston, M. G.; Eisele, F. L.; Ellis, H. W.; McDaniel, E. W. *J. Chem. Phys.* **1977**, *67*, 1276.
(67) Pope, W. M.; Ellis, H. W.; Eisele, F. L.; Thackston, M. G.; McDaniel, E. W.; Langley, R. A. *J. Chem. Phys.* **1978**, *68*, 4761.
(68) Wu, C.; Siems, W. F.; Klasmeier, J.; Hill, H. H. *Anal. Chem*. **2000**, *72*, 391.
(69) Barnett, D. A.; Ells, B.; Guevremont, R.; Purves, R. W. *J. Am. Soc. Mass Spectrom.* **1999**, *10*, 1279.
(70) Handy, R.; Barnett, D. A.; Purves, R. W.; Horlick, G.; Guevremont, R. *J. Anal. At. Spectrom*. **2000**, *15*, 907.
(71) Gabryelski, W.; Froese, K. L. *J. Am. Soc. Mass Spectrom.* **2003**, *14*, 265.
(72) Borysik, A. J. H.; Read, P.; Little, D. R.; Bateman, R. H.; Radford, S. E.; Ashcroft, A. E. *Rapid Commun. Mass Spectrom.* **2004**, *18*, 2229.
(73) Asbury, G. R.; Hill, H. H., Jr. *J. Chromatogr., A* **2000**, *902*, 433.
(74) Lubman, D. M. *Anal. Chem*. **1984**, *56*, 1298.
(75) Rokushika, S.; Hatano, H.; Hill, H. H., Jr. *Anal. Chem*. **1986**, *58*, 361.